# Using $\alpha$ as extrinsic parameter in the template family

Alessandra Buonanno, Yanbei Chen and Michele Vallisneri
(Dated: February 4, 2005)

This note deals with the maximization over the amplitude parameter, $\alpha$, and the orbital phase $\phi$, in the non-precessing BCV template bank. It is based on existing methods of maximization over two angles simultaneously, which has been used in the $\mathcal{F}$-statistic technique for pulsar searches. The additional feature we add here is that we allow the range of $\alpha$ to be specified. We also study false alarm rate in the case of Gaussian noise.

## I. THE TEMPLATE BANK

The Fourier-domain BCV templates are of the form

$$h(f) = \underbrace{f^{-7/6}(1-\alpha f^{2/3})}_{\mathcal{A}(f)} e^{i\phi} \overbrace{e^{2\pi i f t_0 + f^{-5/3}(\psi_0+\psi_{1/2}f^{1/3}+\ldots)}}^{e^{i\psi(f)}}, \quad f>0\,, \tag{1}$$

with $h(f)=h^*(-f)$ for $f<0$. Here we denote by $\mathcal{A}(f)$ the amplitude part of the template. All through this note, we focus on the two *extrinsic parameters*, $\phi$ and $\alpha$.

We first construct an orthonormal basis $\{\hat{h}_j\}$ for the 4-dimensional linear subspace of templates with $\phi\in[0,2\pi)$ and $\alpha\in(-\infty,+\infty)$ but with other parameters fixed. This can be done by constructing two real functions, $\mathcal{A}_1(f)$ and $\mathcal{A}_2(f)$, which are linear combinations of $f^{-7/6}$ and $f^{-1/2}$ (with real coefficients) and satisfy

$$4\int_0^{+\infty} df\,\frac{\mathcal{A}_i(f)\mathcal{A}_j(f)}{S_h(f)} = \delta_{ij}\,. \tag{2}$$

Subsequently, by defining $\hat{h}_{1,2}(f)\equiv\mathcal{A}_{1,2}(f)e^{i\psi}$, $\hat{h}_{3,4}\equiv i\mathcal{A}_{1,2}(f)e^{i\psi}$ for $f>0$ and $\hat{h}_k(f)=\hat{h}_k^*(-f)$ for $f<0$, we will have

$$\langle\hat{h}_i|\hat{h}_j\rangle = \delta_{ij}\,, \tag{3}$$

and hence $\{\hat{h}_j\}$ is the desired basis. Note that $\{f^{-7/6},f^{-1/2}\}$ being real is crucial in the construction of this orthonormal basis. For definiteness, we can choose the following basis functions

$$\begin{bmatrix}\mathcal{A}_1(f)\\ \mathcal{A}_2(f)\end{bmatrix} = \begin{bmatrix}a_{11} & 0\\ a_{21} & a_{22}\end{bmatrix}\begin{bmatrix}f^{-7/6}\\ f^{-1/2}\end{bmatrix} \tag{4}$$

with

$$a_{11}=I_{7/3}^{-1/2}\,,\quad a_{21}=-\frac{I_{5/3}}{I_{7/3}}\left[I_1-\frac{I_{5/3}^2}{I_{7/3}}\right]^{-1/2}\,,\quad a_{22}=\left[I_1-\frac{I_{5/3}^2}{I_{7/3}}\right]^{-1/2}\,. \tag{5}$$

where

$$I_k\equiv 4\int_0^{+\infty}df\,\frac{f^{-k}}{S_h(f)}\,. \tag{6}$$

Now, we can parametrize the *normalized* template using two angles, the orbital phase $\phi$ and an angle $\theta$ [see Eq. (3)],

$$\hat{h}(\theta,\phi;f)=\hat{h}_1(f)\cos\theta\cos\phi+\hat{h}_2(f)\sin\theta\cos\phi+\hat{h}_3(f)\cos\theta\sin\phi+\hat{h}_4(f)\sin\theta\sin\phi\,,\quad (f>0) \tag{7}$$

where $\theta$ is related to $\alpha$ by

$$\tan\theta = -\frac{a_{11}\alpha}{a_{22}+a_{21}\alpha}\,. \tag{8}$$

For any given signal $s$, the overlap is (since normalization of template has already been taken care of)

$$\rho=\langle s|\hat{h}\rangle = x_1\cos\theta\cos\phi+x_2\sin\theta\cos\phi+x_3\cos\theta\sin\phi+x_4\sin\theta\sin\phi\,, \tag{9}$$

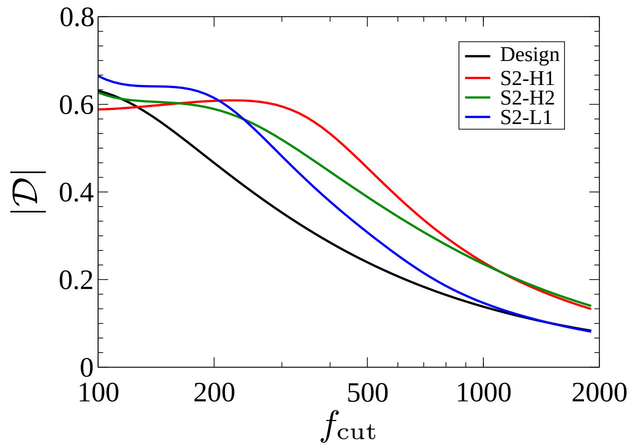


FIG. 1: The angular interval $|\mathcal{D}|$ as functions of $f_{\rm cut}$, for S2 and design-goal noise curves, see Eq. (10).

where $x_k \equiv \langle s|\hat{h}_k\rangle$, $k = 1, 2, 3, 4$, are the only four overlaps we need to compute.

Since $\phi$ is intended for the orbital phase, we must search over the entire $[0, 2\pi)$, while $\theta$ does not need to go through the entire range of $[0, \pi)$, instead, since we have an initial constraint on $\alpha$, namely $0 < \alpha < f_{\rm cut}^{-2/3}$, $\theta$ will be restricted inside an interval, given by Eq. (8), which we denote by $\mathcal{D}$. We now argue that the length $|\mathcal{D}|$ of this interval must be smaller than $\pi/2$. Imagine that we continuously increase $\alpha$ from 0 to $f_{\rm cut}^{-2/3}$, the representation of the template amplitude $\mathcal{A}(f)$ in the $\mathcal{A}_{1,2}$ space will then continuously rotate by $|\mathcal{D}|$ (with its modulus varying continuously). Were the rotation angle in this space to pass through $\pi/2$, say at $\alpha = \alpha_*$, then we must have a vanishing inner product between $\mathcal{A}_{\alpha=0}(f)$ and $\mathcal{A}_{\alpha=\alpha_*}(f)$ — yet this should never happen, because we maintain $\mathcal{A}_\alpha(f) > 0$ all through our range of $\alpha$. As a consequence, $|\mathcal{D}| < \pi/2$. In Eq. (8), this means the denominator $a_{22} + a_{21}\alpha$ does not go through 0 when $\alpha$ varies from 0 to $f_{\rm cut}^{-2/3}$. We then have

$$\mathcal{D} = \left[-\arctan\frac{a_{11} f_{\rm cut}^{2/3}}{a_{22} + a_{21} f_{\rm cut}^{2/3}}, 0\right] \subset (-\pi/2, 0]\,. \tag{10}$$

In Fig. 1, we plot $|\mathcal{D}|$ as a function $f_{\rm cut}$ ranging from 100 Hz to 2000 Hz, using S2 and design-goal noise curves.

## II. ALGEBRAIC MAXIMIZATION OVER $\alpha$

Maximizing (9) over $(\theta, \phi) \in \mathcal{D} \times [0, 2\pi)$, we have

$$\begin{aligned} \rho_{\mathcal{D}} &= \max_{\theta\in\mathcal{D}} \left[(x_1\cos\theta + x_2\sin\theta)^2 + (x_3\cos\theta + x_4\sin\theta)^2\right]^{1/2} \\ &= \max_{\theta\in\mathcal{D}} \frac{1}{\sqrt{2}}\left[V_0 + V_1\cos 2\theta + V_2\sin 2\theta\right]^{1/2}\,, \end{aligned} \tag{11}$$

where

$$\begin{aligned} V_0 &\equiv (x_1^2 + x_2^2 + x_3^2 + x_4^2)\,, \\ V_1 &\equiv (x_1^2 + x_3^2 - x_2^2 - x_4^2)\,, \\ V_2 &\equiv (2x_1x_2 + 2x_3x_4)\,. \end{aligned} \tag{12}$$

From Eq. (11), we note that $\theta \to \theta + \pi$ leaves $\rho_{\mathcal{D}}$ unchanged, so we only need to work with $\theta$ in an interval with length $\pi$.

The maximization of (11) has a geometrical meaning, and is rather straightforward. Suppose $\mathcal{D} = [\theta_a, \theta_b]$, $-\pi/2 <$

$\theta_a < \theta_b \le \pi/2$, then

$$\rho_{\mathcal{D}} = \begin{cases} \frac{1}{\sqrt{2}}\left[V_0 + |\mathbf{V}|\right]^{1/2} & \theta_V \in [2\theta_a, 2\theta_b] \\ \frac{1}{\sqrt{2}}\left[V_0 + \mathbf{V}\cdot(\cos 2\theta_a,\, \sin 2\theta_a)\right]^{1/2} & \theta_V \in [\theta_a+\theta_b-\pi, 2\theta_a] \\ \frac{1}{\sqrt{2}}\left[V_0 + \mathbf{V}\cdot(\cos 2\theta_b,\, \sin 2\theta_b)\right]^{1/2} & \theta_V \in [2\theta_b, \theta_a+\theta_b+\pi] \end{cases}, \tag{13}$$

where have defined

$$\mathbf{V} \equiv (V_1,\, V_2)\,, \quad \theta_V \equiv \arg(V_1 + i\,V_2)\,. \tag{14}$$

In the special (but nonphysical) case of unconstrained $\alpha$, we have $\mathcal{D} = (-\pi/2, \pi/2]$, and Eq. (13) always takes the first case:

$$\rho_{[0,\pi)} = \frac{1}{\sqrt{2}}\left[V_0 + |\mathbf{V}|\right]^{1/2}\,. \tag{15}$$

## III. FALSE ALARM PROBABILITY

In order to estimate the false-alarm probability due to this search, suppose there is only Gaussian noise in $s$, then $x_1, x_2, x_3, x_4$ are independent Gaussian random variables with zero mean and unit variance. The false alarm probability, with a threshold $\rho_*$, can be written as the following:

$$\begin{aligned} \mathcal{F}(\rho_*) &= P\left[V_0 + \max_{\theta\in\mathcal{D}}\left(V_1\cos 2\theta + V_2 \sin 2\theta\right) > 2\rho_*^2\right] \\ &= P\Big[V_0 + |\mathbf{V}| > 2\rho_*^2,\ \theta_V \in [2\theta_a, 2\theta_b]\Big] \\ &+ P\Big[V_0 + |\mathbf{V}|\cos(\theta_V - 2\theta_a) > 2\rho_*^2,\ \theta_V \in [\theta_a+\theta_b-\pi, 2\theta_a)\Big] \\ &+ P\Big[V_0 + |\mathbf{V}|\cos(\theta_V - 2\theta_b) > 2\rho_*^2,\ \theta_V \in (2\theta_b, \theta_a+\theta_b+\pi)\Big]\,. \end{aligned} \tag{16}$$

From Appendix A, we know that $\theta_V$ is statistically independent from both $V_0$ and $|\mathbf{V}|$, and is uniformly distributed over $[0, 2\pi)$, so

$$P\Big[V_0 + |\mathbf{V}| > 2\rho_*^2,\ \theta_V \in [2\theta_a, 2\theta_b]\Big] = \frac{\theta_b - \theta_a}{\pi} P\Big[V_0 + |\mathbf{V}| > 2\rho_*^2\Big] = \frac{|\mathcal{D}|}{\pi} e^{-\rho_*^2/2}\left[\sqrt{\frac{\pi}{2}}\rho_*\,\mathrm{erf}\left[\frac{\rho_*}{\sqrt{2}}\right] + e^{-\rho_*^2/2}\right]\,. \tag{17}$$

[See Appendix B for detailed calculations.] Using results in Appendix A, we can combine the last two lines of Eq. (16) into

$$P\Big[V_0 + |\mathbf{V}|\cos\theta_V > 2\rho_*^2,\ \theta_V \in [-\pi - \theta_a + \theta_b, \pi + \theta_a - \theta_b)]\Big]\,. \tag{18}$$

[In particular, we apply sample-space transformations $T_{\theta_a}$ and $T_{\theta_b}$, respectively, for these two terms, and then use Eqs. (A7), (A8) and (A4).] We have not been able to integrate this analytically, and we give an upper bound here,

$$P\Big[V_0 + |\mathbf{V}|\cos\theta_V > 2\rho_*^2,\ \theta_V \in [-\pi - \theta_a + \theta_b, \pi + \theta_a - \theta_b)]\Big] < P\Big[V_0 + |\mathbf{V}|\cos\theta_V > 2\rho_*^2\Big] = e^{-\rho_*^2/2}\,, \tag{19}$$

and we can write

$$P\Big[V_0 + |\mathbf{V}|\cos\theta_V > 2\rho_*^2,\ \theta_V \in [-\pi - \theta_a + \theta_b, \pi + \theta_a - \theta_b)]\Big] = [1 - \epsilon(\rho_*, \theta_b - \theta_a)]e^{-\rho_*^2/2}\,, \tag{20}$$

where $\epsilon(\rho_*, \theta_b - \theta_a) > 0$ is a correction factor. As we shall see in Appendix C, this correction will always be negligible ($\lesssim 10^{-6}$) for all cases of our interest, with $\rho_* > 5$ and $\theta_b - \theta_a < \pi/2$. Summarizing Eqs. (17) and (20) , we have

$$\begin{aligned} \mathcal{F}(\rho_*) &= [1 - \epsilon(\rho_*, \theta_b - \theta_a)]e^{-\rho_*^2/2} + \frac{|\mathcal{D}|}{\pi} e^{-\rho_*^2/2}\left[\sqrt{\frac{\pi}{2}}\rho_*\,\mathrm{erf}\left[\frac{\rho_*}{\sqrt{2}}\right] + e^{-\rho_*^2/2}\right] \\ &\approx e^{-\rho_*^2/2}\left[1 + \frac{|\mathcal{D}|}{\pi}\sqrt{\frac{\pi}{2}}\rho_*\right]\,, \qquad (\rho_* > 5,\ \theta_b - \theta_a < \pi/2)\,. \end{aligned} \tag{21}$$

Here the first term correspond to the false-alarm probability with only maximization over orbital phase, the second term comes from $\alpha$ maximization. Again, the approximate result in Eq. (21) will have relative error less than the order of $10^{-6}$.

As comparisons, we are also interested in the false-alarm probability with uncontrainted $\alpha$, which can be readily obtained from Eq. (17) by setting $|\mathcal{D}| = \pi$. Now we can put together false-alarm probabilities with unmaximized $\alpha$, physically constrained $\alpha$ [see Eq. (10) and Fig. 1], and unconstrained $\alpha$ (assuming $\rho_* > 5$):

$$\mathcal{F}(\rho_*) = e^{-\rho_*^2/2} \cdot \begin{cases} 1 & \text{unmaximized, } |\mathcal{D}| = 0 \\ 1 + \dfrac{|\mathcal{D}|}{\pi}\sqrt{\dfrac{\pi}{2}}\rho_* & \text{physically constrainted } \alpha,\ 0 < |\mathcal{D}| < \pi/2 \\ \sqrt{\dfrac{\pi}{2}}\rho_* & \text{unconstrained } \alpha,\ |\mathcal{D}| = \pi \end{cases} . \tag{22}$$

Suppose a threshold of $\rho_*^{(0)} = 8.1$ is needed before $\alpha$ is introduced, in order to achieve a certain single-template (i.e., *for a single set of intrinsic parameters* $\psi_{0,1/2,\ldots}$ *and arrival time* $t_0$) false-alarm probability, $P^{(0)}$. Now suppose we search through $\alpha$ in a *physical range* of $|\mathcal{D}| = 0.7$ [see Fig. 1]. Were the threshold to remain the same [$\rho_*^{(0)} = 8.1$], then adding templates (with non-zero $\alpha$) would give a higher single-template false-alarm probability, $3.26\,P^{(0)}$. [Alternatively, one could also regard the constrained search over $\alpha$ as effectively placing 2.26 *extra* independent templates along the $\alpha$ direction.] In order to drive the single-template false-alarm probability back to $P^{(0)}$, $\rho_*$ has to be increased by 1.8%. As a consequence, a 1.8% increase in overlap is required to such a constrained $\alpha$ search. For comparison, an *unconstrained* $\alpha$ search with the same threshold [$\rho_*^{(0)} = 8.1$] will yield a single-template false-alarm probability of $10.2P^{(0)}$, and would require a threshold increase of 3.5% to drive it back.

## APPENDIX A: STATISTICAL INDEPENDENCE BETWEEN $\{V_0, |\mathbf{V}|\}$ AND $\theta_V$

Here we show that $\theta_V$ is statistically independent with the set $\{V_0, |\mathbf{V}|\}$, and that $\theta_V$ is distributed uniformly. We denote

$$(x_1, x_2) \equiv r_A(\cos\theta_A, \sin\theta_A)\,, \quad (x_3, x_4) = r_B(\cos\theta_B, \sin\theta_B)\,, \tag{A1}$$

with $0 \le \theta_A, \theta_B < 2\pi$. It is easy to show that the random variables $\{r_A, r_B, \theta_A, \theta_B\}$ are mutually independent, and that $\theta_A$ and $\theta_B$ are uniformly distributed over $[0, 2\pi)$. For any set $S$, we have

$$\begin{aligned} P\big[S\big] &= \int_S p_{r_A r_B \theta_A \theta_B}(r_A, r_B, \theta_A, \theta_B) dr_A dr_B d\theta_A d\theta_B \\ &= \int_S p_{r_A}(r_A) p_{r_B}(r_B) dr_A dr_B d\theta_A d\theta_B\,, \end{aligned} \tag{A2}$$

due to the independence between $\{r_A, r_B, \theta_A, \theta_B\}$ and the uniformity of distributions of $\theta_A$ and $\theta_B$. We can apply a one-to-one smooth coordinate transformation,

$$\mathcal{T}_\delta : \theta_{A,B} \to \theta_{A,B} + \delta\,, \tag{A3}$$

in the last integral of Eq. (A2) and obtain, by noting that the Jacobian of $\mathcal{T}_\delta$ is identity, and that the probability density does not depend on $\theta_{A,B}$:

$$P\big[S\big] = \int_{\mathcal{T}_\delta(S)} p_{r_A}(r_A) p_{r_B}(r_B) dr_A dr_B d\theta_A d\theta_B = P[\mathcal{T}_\delta(S)]\,. \tag{A4}$$

where $\mathcal{T}_\delta$ is the image of $S$ under $\mathcal{T}_\delta$.

We can express $V_0$, $\mathbf{V}$, and $|\mathbf{V}|$ in terms of $\{r_A, r_B, \theta_A, \theta_B\}$,

$$V_0 = r_A^2 + r_B^2\,, \tag{A5}$$

$$\mathbf{V} = (r_A^2 \;\; r_B^2) \begin{pmatrix} \cos 2\theta_A & \sin 2\theta_A \\ \cos 2\theta_B & \sin 2\theta_B \end{pmatrix}\,, \quad |\mathbf{V}| = \sqrt{r_A^4 + r_B^4 + 2r_A^2 r_B^2 \cos(2\theta_A - 2\theta_B)}\,. \tag{A6}$$

and it is easy to verify that

$$\mathcal{T}(V_0) = V_0, \quad \mathcal{T}_\delta(\mathbf{V}) = \mathbf{V} \begin{pmatrix} \cos 2\delta & \sin 2\delta \\ -\sin 2\delta & \cos 2\delta \end{pmatrix}\,, \tag{A7}$$

and that

$$\mathcal{T}_\delta(|\mathbf{V}|) = |\mathbf{V}|, \quad \mathcal{T}_\delta(\theta_V) = \theta_V + 2\delta\,. \tag{A8}$$

In order to prove independence of $\theta_V$ from $\{V_0, |\mathbf{V}|\}$, the set of our interest is

$$S \equiv \{V_0 \in S_A,\, |\mathbf{V}| \in S_B,\, \theta_V \in [\alpha,\beta)\}\ . \tag{A9}$$

From Eqs. (A7) and (A8),

$$\mathcal{T}_\delta(S) = \{V_0 \in S_A,\, |\mathbf{V}| \in S_B,\, \theta_V \in [\alpha-2\delta,\beta-2\delta)\}\ , \tag{A10}$$

so from Eq. (A4), we have

$$P\big[V_0 \in S_A,\, |\mathbf{V}| \in S_B,\, \theta_V \in [\alpha,\beta)\big] = P\big[V_0 \in S_A,\, |\mathbf{V}| \in S_B,\, \theta_V \in [\alpha-2\delta,\beta-2\delta)\big]\,, \quad \forall \alpha,\beta,\delta\,, \tag{A11}$$

which leads to

$$P\big[V_0 \in S_A,\, |\mathbf{V}| \in S_B,\, \theta_V \in [\alpha,\beta)\big] = P\big[\theta_V \in [\alpha,\beta)\big]P\big[V_0 \in S_A,\, |\mathbf{V}| \in S_B\big] = \frac{\beta-\alpha}{2\pi}P\big[V_0 \in S_A,\, |\mathbf{V}| \in S_B\big]\,, \tag{A12}$$

and hence the independence of $\theta_V$ from $\{V_0, |\mathbf{V}|\}$.

## APPENDIX B: DISTRIBUTION FUNCTIONS OF $V_0 + |\mathbf{V}|$ AND $V_0 + |\mathbf{V}|\cos\theta_V$

In order to calculate the probability density of $V_0 + |\mathbf{V}|$, we write

$$x_{1,4} = \frac{y_1 \pm y_2}{\sqrt{2}}\,, \quad x_{2,3} = \frac{y_3 \pm y_4}{\sqrt{2}}\,, \tag{B1}$$

and

$$A \equiv \sqrt{y_1^2 + y_4^2}\,, \quad B \equiv \sqrt{y_2^2 + y_3^2}\,, \quad V_0 + |\mathbf{V}| = (A+B)^2\,. \tag{B2}$$

This means

$$P\Big[V_0 + |\mathbf{V}| > 2\rho_*^2\Big] = P\Big[A + B > \sqrt{2}\rho_*\Big]\,. \tag{B3}$$

For $A$ and $B$, we have the joint probability density of

$$p_{AB}(A,B) = AB\exp\left(-\frac{A^2+B^2}{2}\right)\,, \quad A, B \geq 0\,. \tag{B4}$$

From this, we deduce

$$P\Big[V_0 + |\mathbf{V}| > 2\rho_*^2\Big] = e^{-\rho_*^2/2}\left[\sqrt{\frac{\pi}{2}}\rho\,\mathrm{erf}\left[\frac{\rho}{\sqrt{2}}\right] + e^{-\rho_*^2/2}\right]\,. \tag{B5}$$

On the other hand, because $V_0 + |\mathbf{V}|\cos\theta_V = V_0 + V_1 = 2x_1^2 + 2x_3^2$, it is obvious that

$$P\Big[V_0 + |\mathbf{V}|\cos\theta_V > 2\rho_*^2\Big] = P[x_1^2 + x_3^2 > \rho_*^2] = e^{-\rho_*^2/2}\,. \tag{B6}$$

## APPENDIX C: FULL CALCULATION OF THE PROBABILITY (18)

From Eqs. (B2) and (B4), it is straightforward to obtain the joint probability density of $\{V_0, |\mathbf{V}|\}$:

$$p_{\{V_0,|\mathbf{V}|\}}(x,y) = \frac{y e^{-x/2}}{4\sqrt{x^2-y^2}}\,, \quad x > y > 0\,. \tag{C1}$$

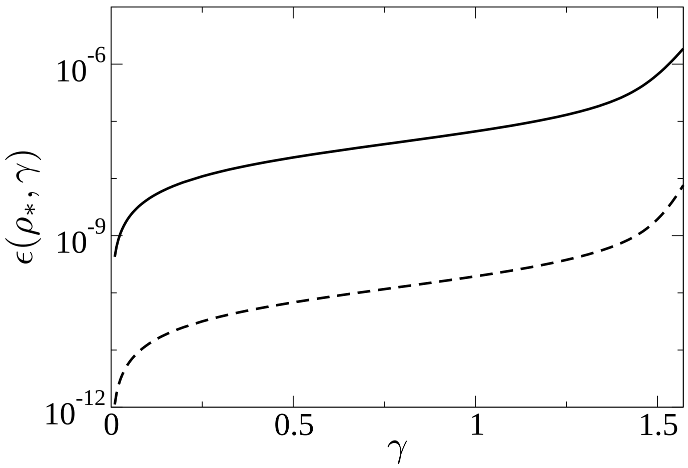


FIG. 2: The correction factor $\epsilon(\rho_*, \gamma)$ for $0 < \gamma < \pi/2$ and $\rho = 5$ (solid curve) and 6 (dashed curve).

We then have

$$(18) = P\Big[V_0 + |\mathbf{V}|\cos\theta_V > 2\rho_*^2,\ \theta_V \in [-\pi - \theta_a + \theta_b, \pi + \theta_a - \theta_b)]\Big]$$
$$= \int_{-\pi+\gamma}^{\pi-\gamma} \frac{d\theta}{2\pi} \int\limits_{\substack{x>y \\ x+y\cos\theta > 2\rho_*^2}} dxdy \frac{ye^{-x/2}}{4\sqrt{x^2-y^2}} \tag{C2}$$

where $\gamma \equiv \theta_b - \theta_a$. For $\gamma > 0$, we have not been able to evaluate the above integral analytically. However, because of the factor $e^{-x/2}$, it does seem that the integral over $\theta$ should get most of its contributions from $\theta < \pi/2$, so for small $\gamma$ this integral should not be so different from its value at $\gamma = 0$, which has been given by Eq. (B6). To parametrize the error made by assuming $\gamma = 0$, we have defined a relative error $\epsilon$ in Eq. (20). Here we express it in terms of numerical integrations:

$$\epsilon(\rho_*, \theta_b - \theta_a) = \epsilon(\rho_*, \gamma) = 1 - \int_{-\pi+\gamma}^{\pi-\gamma} \frac{d\theta}{2\pi} \int\limits_{\substack{x>y \\ x+y\cos\theta > 2\rho_*^2}} dxdy \frac{ye^{(\rho_*^2 - x)/2}}{4\sqrt{x^2-y^2}} \tag{C3}$$

$$= 1 - \int_{-\pi+\gamma}^{\pi-\gamma} \frac{d\theta}{2\pi} \left[(1+\rho_*^2)e^{-\rho_*^2/2} + \int_{\frac{2\rho_*^2}{1+\cos\theta}}^{2\rho_*^2} dx \frac{e^{(\rho_*^2 - x)/2}}{4} \sqrt{x^2 - \left(\frac{x - 2\rho_*^2}{\cos\theta}\right)^2}\,\right] \tag{C4}$$

In Fig. 2, we plot $\epsilon(\rho_*, \gamma)$ for $0 < \gamma < \pi/2$ in the cases of $\rho = 5$ and 6. This suggests that in regimes of our interest we can safely ignore $\epsilon$.